Key Engineering Materials
ISSN: 1662-9795, Vol. 809, pp 183-189
doi:10.4028/www.scientific.net/KEM.809.183

Submitted: 2019-01-29
Revised: 2019-02-15
Accepted: 2019-02-25
Online: 2019-06-27

One-Sided Resistance Spot Welding of Plastic-Metal Hybrid Joints - Characterization of the Joining Zone

Konstantin Szallies[1,a*], Michael Friedmann[1,b],
Martin Bielenin[2,c] and Jean Pierre Bergmann[1,b]

[1]Technische Universität Ilmenau, Department of Production Technology, Gustav-Kirchhoff-Platz 2, 98693 Ilmenau (Germany)

[2]Nemak Europe GmbH, The Squaire 17 – Am Flughafen, 60549 Frankfurt/Main (Germany)

[a]*konstantin.szallies@tu-ilmenau.de, [b]info.fertigungstechnik@tu-ilmenau.de, [c]Martin.Bielenin@nemak.com

Keywords: resistance spot welding; resistance spot joining; lightweight design; joining plastics; hybrid structures, metal-plastic hybrid joints

Abstract. Polymer-metal-hybrid components show a high potential regarding to lightweight applications. In particular, due to their fundamental differences in chemical and physical properties, new approaches must be developed for common industrial joining processes. In this study a new approach in order to characterize the joining zone formation for thermal direct joining based on resistance spot welding is reported. The feasibility of joining in half-section set-up using a coaxial electrode arrangement was investigated. The impact of the welding parameters on the joining zone formation was investigated. The parameters influencing the melting layer formation were pointed out.

Introduction

The use and the advancement of constructive and material lightweight principles are essentially in order to achieve the ambitious aims for the reduction of resource consumption in various industries. The current development confirms more and more the importance of mixing different materials with various characteristics. While in case of joining metals to each other, such as for example aluminum to steel and copper to aluminum the formation of intermetallic compounds is a sophisticated target, new and completely different challenges occur in metal-plastic joints, which turn to be a very interesting topic in research and development at the moment. Due to fundamental differences in chemical and physical properties, the challenge is to find new approaches for common joining processes. Currently, these material combinations are joined by mechanical processes or adhesive bonding. However, mechanical joining processes exhibit several disadvantages, especially notches and stress peaks. Curing times of adhesives are considered as a drawback for industrial application as well. In particular thermal joining processes provide several benefits compared to the represented disadvantages.

These processes are principally based on heating the metal partner until the thermoplastic partner melts at the boundary layer, due to heat conduction. The molten polymer wets the surface of the metallic partner and penetrates into eventually present dimples on the surface. After cooling a solid joint occurs. Therefore, different process strategies for heating can be used to achieve polymer-metal hybrid joints, such as thermal direct joining [1, 2], ultrasonic joining [3, 4], induction joining [5, 6], infrared radiation [7], laser joining [8, 9, 10] or resistance joining [11, 12, 13].

Resistance spot welding is still the most common technology in the sheet-metal working industry for joining. In particular, this is caused by minor process costs and a short welding times. Common resistance spot welding requires a both sided accessibility. Therefore resistance spot joining of polymer-metal hybrid components is not possible. One-sided resistance welding is considered in this paper as novel technology for join polymer-metal hybrid structures.

The process observation of resistance spot welding is a crucial challenge, due to the fast process conditions and the hidden joint formation between the electrodes. Authors such as [14], [15] or [16] use a halved electrode assembly in conjunction with a high-speed camera, as shown in Figure 1 b. Due to this setup it is possible to provide information related to melting and solidification of the welding spot as well as the temperature distributions within the welding spot for metal/metal joints. [15][16].

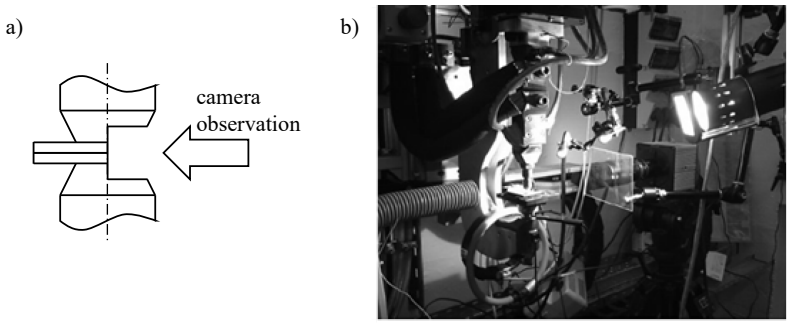

Fig. 1: (a) Half-section configuration of [14]; (b) half-section camera observation set-up of [15]

Experimental Setup

The experimental investigations were carried out using a 50 Hz alternating current projection welding machine (Dalex PMS 11-4). Due to the isolating properties of the polymer, a one-sided electrode arrangement was used. Regarding to common automotive flange geometries and working areas a special device for welding with a coaxial electrode arrangement was designed by the authors within the TU Ilmenau. The schematic configuration of the device is shown in figure 2 a. The external ring electrode is arranged as circular ring with an outside diameter of 16 mm. The internal welding electrode was chosen according to DIN EN ISO 5821-F1 geometry. Due to the coaxial arrangement the diameter of the internal electrode should not exceed 10 mm, therefore a down scaling of the standardized diameter was necessary. Both electrodes were manufactured out of a CuCr1Zr-alloy in order to use a common electrode material. The total welding force (F_{total}) of the projection welding machine is divided into the inner welding electrode force (F_{in}) and the outer ring electrode force (F_{ring}) through setting a spring, in order to allow the external electrode to take contact to the material first and then moving the internal electrode to the material.

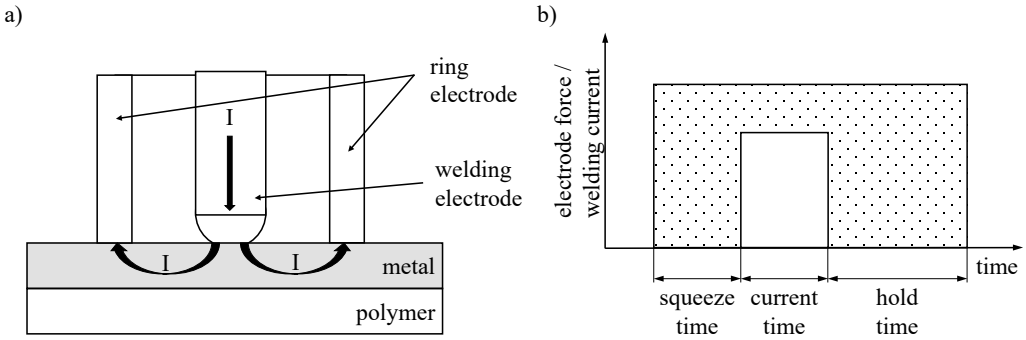

Fig. 2: (a) Schematic configuration of the welding tool; (b) used welding cycle

The used welding cycle is schematically shown in figure 2b. After iterative preliminary investigations, the welding parameters ring electrode force (F_{ring} = 1320 N), squeeze time (200 ms) and hold time (1000 ms) were kept constant. For the investigations due to the characterization of the melt formation the device was adapted to a half section model. Based on the half section set-up of Schneemann [14] both electrodes were halved 7 mm above the working area. The workspace configuration is shown in figure 3 a. The electrodes of the realized welding tool are shown by the ring- and the welding electrode. The metal and the polymer sheets are arranged below. A common automotive steel DX56D and a natural not-dried polyamide 6.6 was selected. The clamping fixes the glass cover, which allows the process monitoring by using a high-speed camera.

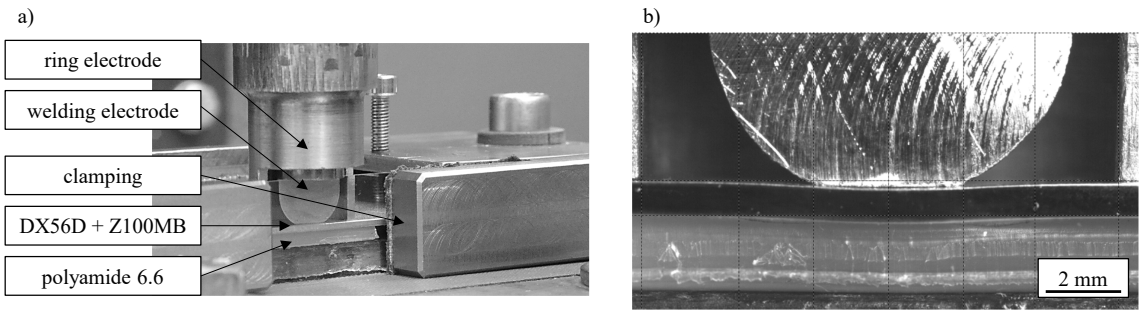

Fig. 3: (a) Workspace configuration; (b) Frame of a high-speed record

Figure 3b shows the arrangement by one frame of a high speed record. In order to achieve a planar and sealed positioning of the sheet, the metal edge was flat grinded up to a grain size of 2000. After shear cutting the polymer edge received no additional process. To avoid a preferred direction of the molten polymer, the surface of the metal was not structured. Figure 4 shows the used specimen geometry based on [13]. The overlap was 20 mm.

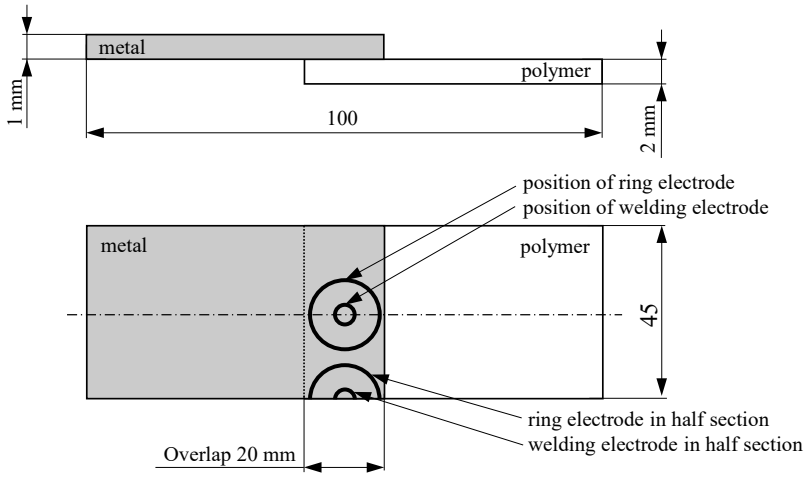

Fig. 4: Specimen geometry and electrode working area

For the investigations in the context to the half section model a high-speed camera Optronis CR3000x2 with a macrolens was used. The frame rate was 1000 fps. The temperature field was observed with a thermometry camera InfraTec Image IR 8300. Using a frame rate of 100 fps.

Results and Discussion

Evaluation of the half-section setup

The half-section investigation was carried out based on Schneemann's [14] set-up. In contrast to [13] the contacting cross-section area is halved, as a result the current density and the surface pressure increases. Therefore preliminary investigation to evaluate process conditions using weldability lobes are necessary. The resulting weldability lobes in dependency of the electrode force are shown in figure 5. Common test and documentation guidelines to determinate weldability lobes could not be assigned for half-section set-up. In deviation to DIN EN ISO 14327 the minimum process limit of the weldability lobes were defined by a visible thermal influence of the polymer. The maximum process limit was defined by a thermal degradation of the polymer. The characteristic weldability lobes show a small welding current range of at most 1 kA in the range of 200 ms to 600 ms. Increasing electrode forces enables a more pronounced current range. For these investigated electrode forces below welding times of 400 ms, welding currents in the same order of magnitude are necessary.

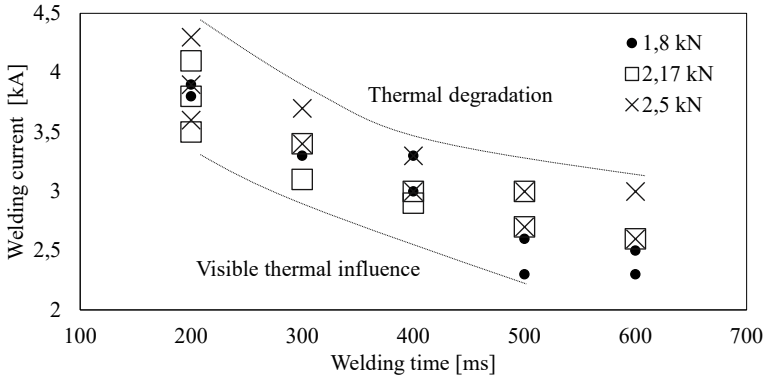

Fig. 5: Weldability lobes in half section configuration in dependency of the electrode force

Joining zone formation

The high-speed recording, allows a process monitoring regarding to the melting layer thickness evolution and the melting layer radius of the polymer. Figure 6 a shows the thermal influenced area in a frame of a high speed record. Basically, as expected, the molten area is characterized by a specific form following the heat input respectively the current path. This methodology allows it to evaluate the influence of process conditions on the geometry of the molten area.

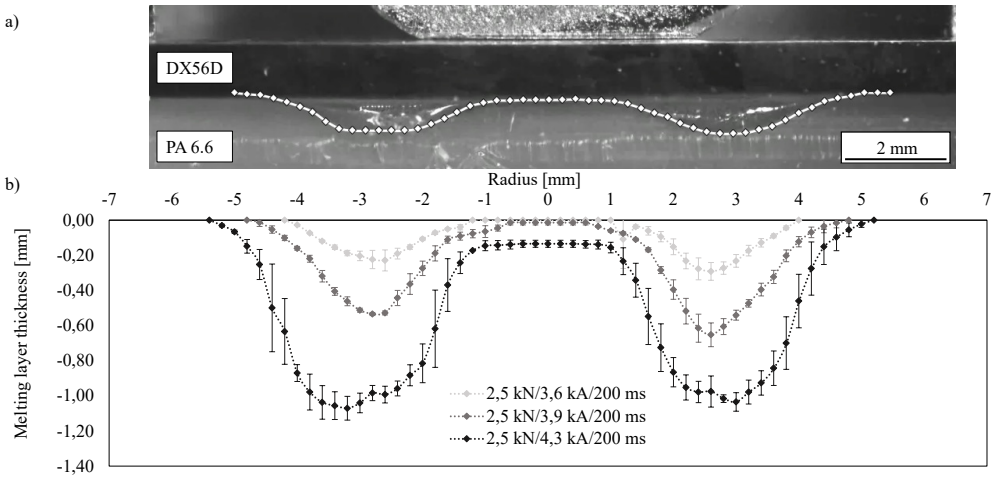

Fig. 6: Thermal influence of the polymer: (a) Image of a high speed record; (b) compared welding currents

The influence of the welding current is shown in Figure 6 b. It can be stated that the welding current affects the melting layer geometry in three ways. Due to the Joule heating resulting from an increasing welding current an increasing spot radius with a deeper layer thickness was detected concurrently a shift of the maximum depth towards higher radius occurs (from 2,6 mm to 3,5 mm). In addition, a plateau in the range of approximately -1 mm to 1 mm distance from the center could be observed. In particular, the actively cooled electrode and the high thermal conductivity of the copper electrode cause only a small melting layer up to 0,2 mm in this area. The process variables welding time and welding force lead to comparable effects. An increasing welding time leads to an enlargement of the melting layer, whereas an increasing electrode force causes a reduction of the melting zone.

Due to the half-section configuration a characterization of the melting process was possible. The current time starts at 0 ms (Figure 7 a). As shown in Figure 7 b at 20 ms a melt front is formed starting from the outer edge of the inner welding electrode. After further propagation of the melting layer, a bubble can be observed (45 ms) at the outer edge of the electrode working area of the inner welding electrode as well. In addition, for increasing welding currents and welding times, the zinc coating of the steel sheet is molten and constraint in the melting layer. The welding time ends after 200 ms. The melting zone is formed as a liquified ring around the inner welding electrode.

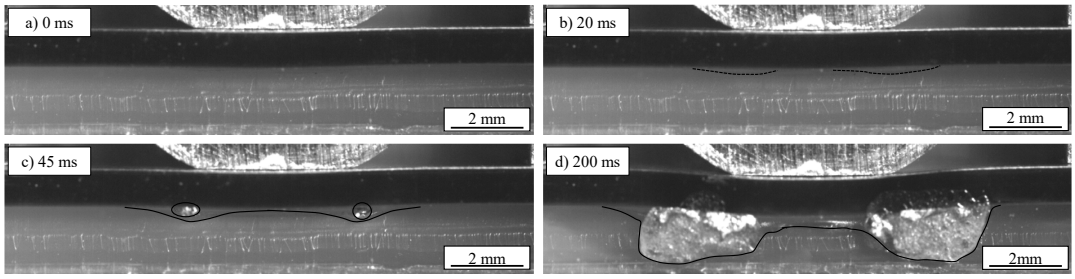

Fig. 7: Melting layer for heating (F=2,17 kN | I=4,1 kA | t=200 ms)

Figure 8 shows a characteristic cooling sequence from the end of the welding time to solidification of the plastic partner during the hold time. In Figure 8 a (+0 ms) the current flow is ending. After 220 ms holding time (Figure 8 b), the melt starts solidifying below working area of the inner electrode, due to the active cooling. Simultaneously the solidification starts at the respective outer layer of the melting zone. In Figure 8 c (560 ms) the solidification continues and only little isles of liquid material are present. The melting layer is completely solidified after 920 ms. The time for solidification depends on the cross-section area of the melting zone. It can be assumed that the material begins and ends to melt at the outer edge, where the electrode working area is in contact with the sheet.

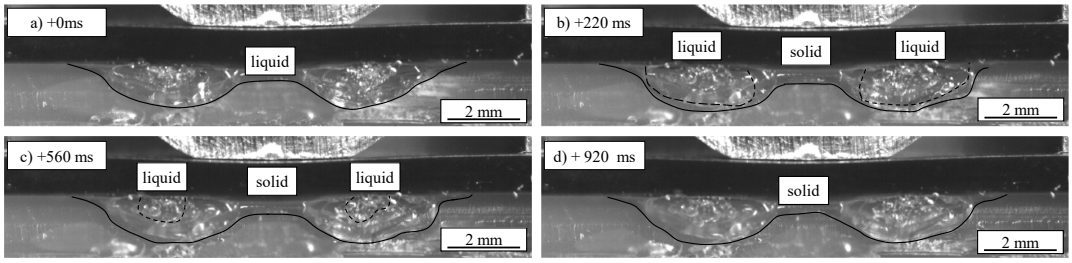

Fig. 8: Melting layer for cooling

Figure 9 shows the results of the temperature distributions measurement of the welds. The process conditions correspond to Figure 7. The horizontal line shows the boundary between metal and plastic and the vertical line represents the outer edge of the inner electrode working area. As shown in the high-speed records, it can be assumed that the maximum process temperature could be determined in this area as here the higher current density is present. After a current time of 170 ms, a maximum temperature of 402 °C is reached at the boundary layer and corresponds approximately to the melting temperature of the zinc coating. After 200 ms the current time ends. The maximum temperature of 546 °C can be measured. The temperature distribution during cooling remains comparable to heating. This reflects the resulting geometry shown in the high speed records. At the outer edge of the electrode working area, the respective temperature maxima occur.

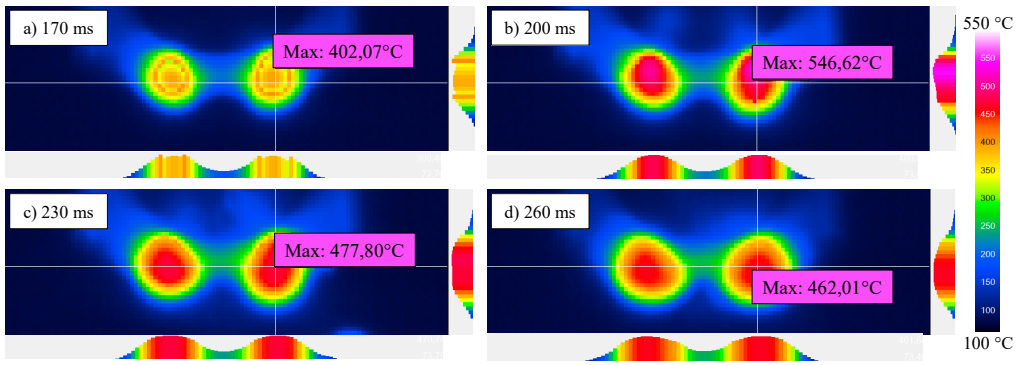

Fig. 9: Temperature distributions in half section set-up (F=2,17 kN | I=4,1 kA | t=200 ms)

Summary

In this paper, novel results regarding to resistance spot joining in half-section configuration of polymer-metal hybrid joints in a coaxial electrode arrangement are reported. Based on preliminary investigation, the process limits were characterized. Moreover, the influence of process variables on the joint formation, especially current was shown. It was pointed out, that the melting layer forms a coaxial nugget around the inner welding electrode. Using high-speed records the moistening as well as the flow and the solidification of the melting layer was characterized. It was shown that the solidification may be regarded as contrary to the heating processes. Particularly the temperature distribution reflects the resulting geometry.
The presented results regarding single side resistance spot joining of polymer-metal-hybrid structures in half-section configuration contribute to a better understanding of the joint formation.

References

[1] Sickert, M.; Haberstroh, E.: Thermal Direct Joining for Hybrid Plastic Metal Structures. In: Proceedings of Euro Hybrid Materials and Structures, (2014) pp. 42-45 .

[2] Flock, D.: Wärmeleitungsfügen hybrider Kunststoff-Metall-Verbindungen. Aachen: Rheinisch-Westfälische Technische Hochschule. Dissertation, 2011.

[3] Balle, F.; Eifler, D.: Monotonic and Cyclic Deformation Behavior of Ultrasonically Welded Hybrid Joints between Light Metals and Carbon Fiber Reinforced Polymers (CFRP). Fatigue Behaviour of Fiber Reinforced Polymers. In: DEStech Publications, (2012) pp. 111-122.

[4] Balle, F.; Wagner, G.; Eifler, D.: Ultrasonic spot welding of aluminum sheet/carbon fiber reinforced polymer-joints. In: Materialwissenschaft und Werkstofftech. 38 (11) 2007 pp. 934-938.

[5] Bobzin, K.; Theiß, S. et.al.: Der Exzellenzcluster "Integrative Produktionstechnik für Hochlohnländer" der RWTH Aachen University - Herstellung hybrider Metall-Kunststoffbauteile durch moderne Fügeverfahren. In: Joining Plastics, 3 (2008) pp. 210-216.

[6] U. Reisgen, S. Olschok, N. Wagner: Neue Entwicklungen zu Verbindungen von Kunststoff und Metall unter Zuhilfenahme thermischer Fügeprozesse. In: 17. Symposium Verbundwerkstoffe und Werkstoffverbunde, (2009) pp. 542-548.

[7] Amend, P.; Pfindel, S.; Schmidt, M.: Thermal joining of thermoplastic metal hybrids by means of mono- and polychromatic radiation. In: Physics Procedia 41, (2013) pp. 98-105.

[8] Schricker, K.; Diller, S.; Bergmann, J. P.: Bubble Formation In Thermal Joining Of Plastics With Metals. In: LANE 2018, 10th Conference on Photonic Technologies.

[9] Schricker, K.; Stambke, M.; Bergmann, J. P.: Macroscopic Surface Structures For Polymer-Metal Hybrid Joint. In: Procedia CIRP 74, 518-523, 2018.

[10] Katayama, S.; Kawahito, Y.; Mizutani, M.: Latest progress in performance and understanding of laser welding. Physics Procedia 39, (2012) pp. 8-16.

[11] Ageorges, C.; Ye, L.: Resistance Welding of Metal/Thermoplastic Composite Joints. Journal of Thermoplastic Composite Materials, Vol. 14, No. 6, (2006) pp. 449-475.

[12] Reisgen, U.; Schiebahn, A.; Schönberger, J.: Innovative Fügeverfahren für hybride Verbunde aus Metall und Kunststoff. In: Lightweight Design, Bd. 7, No. 3 (2014) pp. 12-17.

[13] Szallies, K.; Bielenin, M; Bergmann, J. P., Neudel, C.: Single Side Resistance Spot Welding With A Coaxial Electrode Arrangement For Joining Plastic-Metal-Hybrid Structures. In: Hybrid Materials and Structures 2018.

[14] Schneemann, K.: Vorgänge beim Punktschweißen von Tiefziehstahl und ihr Einfluss auf das Schweißgut, Dissertation, Universität Hannover, 1967

[15] Pepke, L.-A.: Untersuchung der Anlagenkonfiguration beim Widerstands-punktschweißen von Stahlfeinblechen. Berlin, Techn. Univ., F. Dissertation, 2014.

[16] Cho, Y.; Rhee, S.: Experimental Study of Nugget Formation in Resistance Spot Welding. In: Welding Journal (2003), S. 195-201.